Journal of
Computational and Theoretical Nanoscience
Vol. 4, 1108–1119, 2007

RESEARCH ARTICLE

Novel Nanotube-Coordinated Platinum Complexes

Charles See Yeung, Lei Vincent Liu, and Yan Alexander Wang*

Department of Chemistry, University of British Columbia, Vancouver, BC V6T 1Z1, Canada

Pt-doped (5,5) single-walled carbon nanotubes have been studied within density functional theory using a model system consisting of a single Pt center in a symmetrical nanotube segment with capping H atoms. The geometric and electronic properties of this hypothetical material have been investigated. Our calculations suggest a strong affinity of the Pt atom localized within the supramolecular nanotube framework for carbon monoxide. This proposed adsorption process takes place exothermically and yields a new type of nanotube-coordinated organometallic complex similar to classical alkylplatinum species bearing the CO ligand. In this case, however, three coordination sites of the Pt locus are essentially fixed by the backbone of the carbon nanotube and disconnection is unlikely. Metal doping of pure single-walled carbon nanotubes and subsequent adsorption of small molecules may lead to facile control of the fundamental characteristics of these materials. Unprecedented chemical reactivities may also be achieved through a novel possible mechanism coupling elements of surface catalysis with transition-metal mediated transformations.

Keywords: Single-Walled Carbon Nanotube, Doping, Platinum, Adsorption.

1. INTRODUCTION

Iijima's initial discovery of carbon nanotubes in 1993[1] has since prompted experimental and theoretical scientists alike to investigate the utility of these structures as materials. In particular, single-walled carbon nanotubes (SWCNTs) have been explored in regards to their geometric and electronic properties.[2–6] These structures have been used in a variety of disciplines, including application in the crystallization of H_2SO_4,[7] binding of deoxyribonucleic acid (DNA),[8] modification of the electrochemistry of cytochrome *c*,[9] and even hydrogen storage.[10] SWCNTs are typically classified as either metallic or semiconducting,[11] and its electronic properties can be manipulated by either doping[12] or functionalization.[13–17] Herein, we envision a novel type of doping of nanotubes—the incorporation of a transition metal atom into the supramolecular carbon framework.

The local structure of carbon atoms within the nanotube framework resembles that of both graphite and fullerenes, two other known allotropes of carbon. While graphite consists of infinite sheets of sp^2-hybridized carbon atoms with long-range delocalization of π electrons parallel to the plane, both nanotubes and fullerenes exhibit curvature. Concerning fullerenes, it has been shown that cage substitution may take place whereby a single carbon atom is replaced by a transition metal atom.[18–22] For instance, evaporation of pure Fe, Co, Ni, Rh, or Ir into fullerene vapor produces externally-doped metallofullerenes which at substantial temperatures results in substitutional doping.[18] Laser ablation of electrochemically deposited films of C_{60} and $Ir(CO)_2Cl$(*p*-toluidine) or $PtCl_2(pyridine)_2$ gives the Ir and Pt-doped fullerenes, respectively.[19] Similar conditions may be applied to externally-doped species to give the corresponding metallofullerenes with incorporation of Pt, Ni, and Sm.[20]

Extensive density functional theory (DFT) calculations on metallofullerenes[20–22] have yielded predictions in good accord with experiment[22] and provided new insight into the geometrical aspects of metal-substitution for these nanostructures. Interestingly, the inclusion of a transition metal into the carbon framework of pure C_{60} results in a decrease in the energy gap between the highest occupied molecular orbital (HOMO) and the lowest unoccupied molecular orbital (LUMO), thus suggesting both higher conductivity[22] and reactivity.[21]

Inspired by these studies, we decided to examine transition-metal doped SWCNTs. Although experimentally, the doping of carbon nanotubes has not been achieved, we believe that this initial study will provide inorganic and physical chemists alike with a new insight into the chem-

*Author to whom correspondence should be addressed.

1546-198X/2007/4/1108/012 doi:10.1166/jctn.2007.003

ical and material properties of this new substance. Metal-doped SWCNTs may be viewed from two perspectives. On the one hand, from the standpoint of the metal, the supramolecular carbon framework acts as a ligand that essentially rigidifies the transition metal center. Unlike classical organometallic ligands, a nanotube-coordinated species is expected to display different reactivities due not only to the steric size of the carbon framework but also the interaction between the delocalized π electrons along the backbone of the nanotube and the metal d-orbitals and subsequent effect on the local density of electrons on the metal center. On the other hand, from the standpoint of the carbon atoms along the nanotube, the presence of a transition metal atom is an impurity that should affect the mechanical and electronic characteristics of this material. For instance, we might expect that the doping of a transition metal atom might enhance the conductivity along the axis of the nanotube due to the presence of low-lying d-orbitals within the delocalized π-system of the carbon atoms. In addition, the adsorption of small gases onto a metal-doped system is predicted to be starkly different from that of a pure SWCNT. *Combining these two elements, the resulting system effectively spans fields of homogeneous and heterogeneous catalysis and hence makes the hypothetical proposed system an important one to study even if only through calculation.*

We opted to choose Pt for our investigation due to its prevalence in many organometallic complexes,[23–27] the properties of which have been studied extensively by both experiment and theory. In addition, physical chemists have shown that Pt surfaces can adsorb small gas molecules without much difficulty through interaction of the aforementioned metal d-orbitals.[28–31] Previous work in our group on nanorods have suggested an increase in the HOMO–LUMO gap upon Pt-doping of a pure C_{170} system,[32] contrary to that reported for fullerenes. We now disclose further studies on the structural and electronic properties of metal-doped SWCNTs and the effects of carbon monoxide adsorption onto the metal center as assessed by frontier molecular orbital (FMO) and local density of states (LDOS) analyses.

2. THEORETICAL CALCULATIONS

A (5,5) armchair metallic SWCNT fragment with H atoms at the termini ($C_{70}H_{20}$) was chosen as the model for density functional studies. A single carbon atom in the middle of the nanotube was replaced with a Pt atom to produce a segment of a Pt-doped carbon nanotube ($C_{69}H_{20}Pt$). The exchange-correlation density functional of Perdew, Burke, and Ernzerhof (PBEPBE)[33] was employed using the relativistic effective core pseudopotential of Hay and Wadt (LANL2).[34] Geometry optimizations were performed first using the smaller LANL2MB basis set and refined with the larger LANL2DZ basis (Dunning/Huzinaga valence double zeta for first-row elements and Los Alamos ECP plus double zeta for heavier elements).[35] Natural bond orbital (NBO) calculations were done using Gaussian NBO Version 3.1.[36,37] LDOS studies were performed using PyMOlyze.[38] All other calculations were performed using the Gaussian 03 quantum chemical package.[39]

Because spin-restricted and spin-unrestricted optimizations yielded the same result, we concluded that the Pt-doped SWCNT fragment exhibits a closed-shell singlet ground state. Further investigations showed that a low-lying triplet state exists 0.41 eV above the ground state, implying that a bulk amount of the metal-doped nanotube should exist in a statistical distribution of the two spin states as described by Boltzmann assuming facile interconversion between the two states. Consequently, our studies focused on both singlet and triplet states of the adsorbate-nanotube complexes. All open-shell species were treated with spin-unrestricted DFT.

3. RESULTS AND DISCUSSION

3.1. Pt-Doped SWCNTs

The optimized geometries of the model singlet Pt-doped SWCNT systems are shown in Figure 1(a). The Pt atom protrudes to the exterior of the wall and appears to favor a conformation where the three nearest neighbor carbon atoms are positioned in a tripod-like fashion, due to the larger size of the Pt atom. This type of arrangement is in agreement with those previously reported from our group.[32] The Pt—C bond distances in this complex are 1.94, 1.94, and 2.01 Å, respectively. As is the case for metal-doped fullerenes,[18,22] these values are significantly longer than that of the PtC molecule (cf. 1.73 Å), which suggests a weaker Pt—C bond for the Pt-doped SWCNT than that found for PtC.

An NBO partial charge analysis shows that a positive charge of 0.83 remains on the Pt center whose electron configuration is essentially $[Xe]6s^{0.51}5d^{8.67}$. The three neighboring carbon atoms bear negative charges of −0.15, −0.13, and −0.13, respectively. In comparison, the triplet case yields an almost identical geometry and a charge of 0.84 on the Pt atom with electron configuration $[Xe]6s^{0.45}5d^{8.71}$.

The gap between the energies of the HOMO and the LUMO are 0.74 and 0.39 eV for singlet and triplet states, respectively. The smaller transition gap for the triplet Pt-doped SWCNT implies that the conductivity is higher than that of the ground state complex. The LDOS and the overall density of states (DOS) of the singlet and triplet are very similar with only a few minor differences (see appendix).

3.2. Adsorption of CO

As mentioned above, the adsorption of CO on Pt surfaces has been studied by many research groups.[28–31] In addition,

RESEARCH ARTICLE

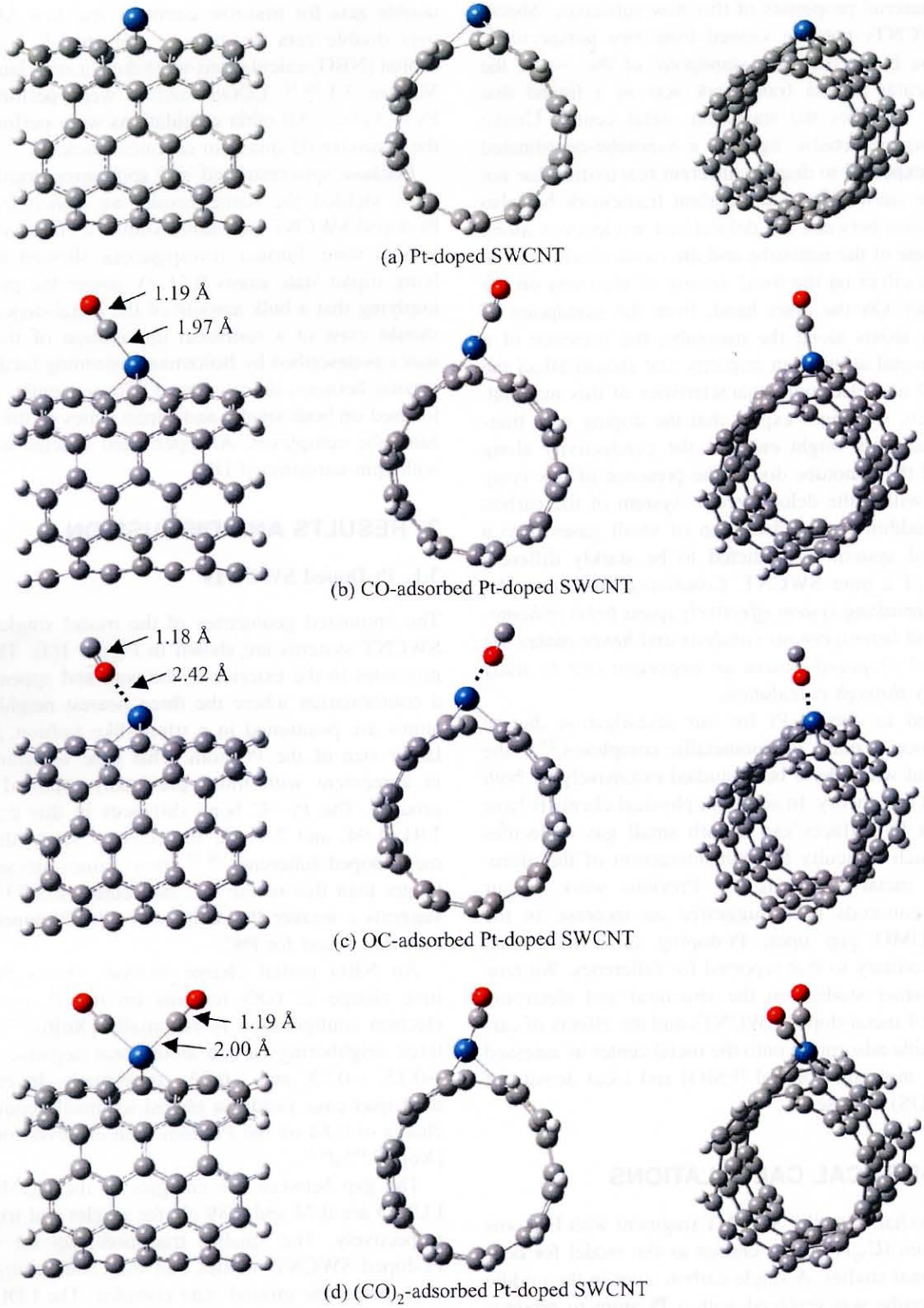

Fig. 1. Optimized geometries for the adsorption of CO onto the Pt-doped SWCNT (grey = C, white = H, blue = Pt, red = O). From left to right, these are views perpendicular to the nanotube axis, along the nanotube axis, and a 3D perspective viewpoint.

CO often serves as an auxiliary ligand for a wide range of organometallic complexes.[23, 24, 26, 27, 40] With both of these in mind, we now turn our attention to the adsorption of carbon monoxide onto Pt-doped SWCNTs.

The most sensible approach is to allow the carbon end of the CO molecule to adsorb to the metal center, forming what we will refer to as the CO-adsorbed Pt-doped SWCNT. Under this assumption, we found that

the adsorption of the first molecule of carbon monoxide is exothermic. For the bare singlet Pt-doped nanotube, 41.23 kcal/mol is liberated upon the complexation, whereas 42.61 kcal/mol is released from the corresponding triplet structure. Geometrically, the SWCNT tends to adopt an asymmetric arrangement whereby the adsorbate is tilted to the side instead of resting on an axis perpendicular to the nanotube axis (see Fig. 1(b)).

Chemisorbed carbon monoxide is usually described by a simple molecular orbital picture.[41] The lone pair of electrons on the carbon that resides in an sp_z-hybrid orbital donates electron density into an appropriate acceptor such as a metal d orbital. The result is a coordinate bond where both electrons involved in the connection are formally from the donor.[42] The consequence, however, is excess electron density on the metal which then back donates from the metal d-orbital to the π^*-orbital of the adsorbate.[40–42] As a result, we would expect a lengthening of the C≡O triple bond and a net negative charge on CO.[40, 42] Indeed, from the NBO analysis, the Pt center now has a 0.85 positive charge, while the carbon and oxygen of the adsorbed carbon monoxide carry charges of 0.28 and −0.41, respectively. The net charge on the adsorbate is −0.12, which signifies a net back donation from the d-orbitals of the Pt atom across the C≡O triple bond. The bond length of the CO is slightly elongated to 1.19 Å (cf. 1.18 Å in the free gaseous molecule). The electron configuration of the Pt center is $[Xe]6s^{0.5}5d^{8.65}$.

It should be noted that the molecular orbitals bear great resemblance to unperturbed d orbitals about the Pt center (see Fig. 2(c)). However, it is evident that electron density is delocalized about the extended carbon framework. Overall, the HOMO–LUMO gap is decreased from 0.74 to 0.58 eV for the singlet. The triplet scenario also shows similar C≡O bond length (1.20 Å), partial charges (Pt: 0.83, C: 0.26, O: −0.42), and Pt electron configuration ($[Xe]6s^{0.46}5d^{8.70}$), but unlike the ground state, the HOMO–LUMO gap is increased to 0.56 eV from 0.39 eV.

One obvious question is whether or not our initial assumption of adsorption via the carbon atom is correct. Since the Pt-doped SWCNT is a new type of

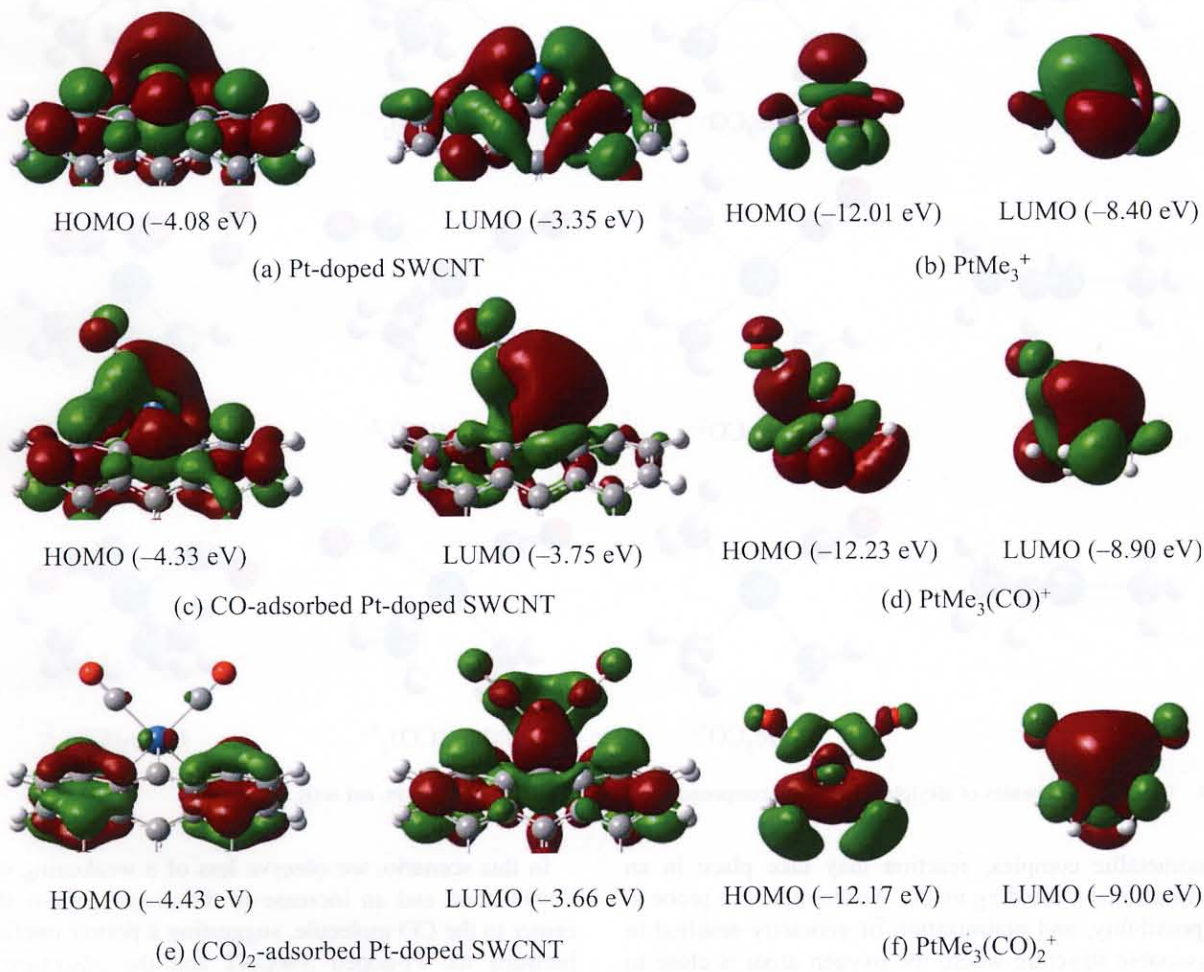

Fig. 2. Frontier molecular orbitals for the alkylplatinum complexes and the Pt-doped SWCNT. HOMO (p eV) is the highest occupied molecular orbital with energy p eV. LUMO (q eV) is the lowest unoccupied molecular orbital with energy q eV.

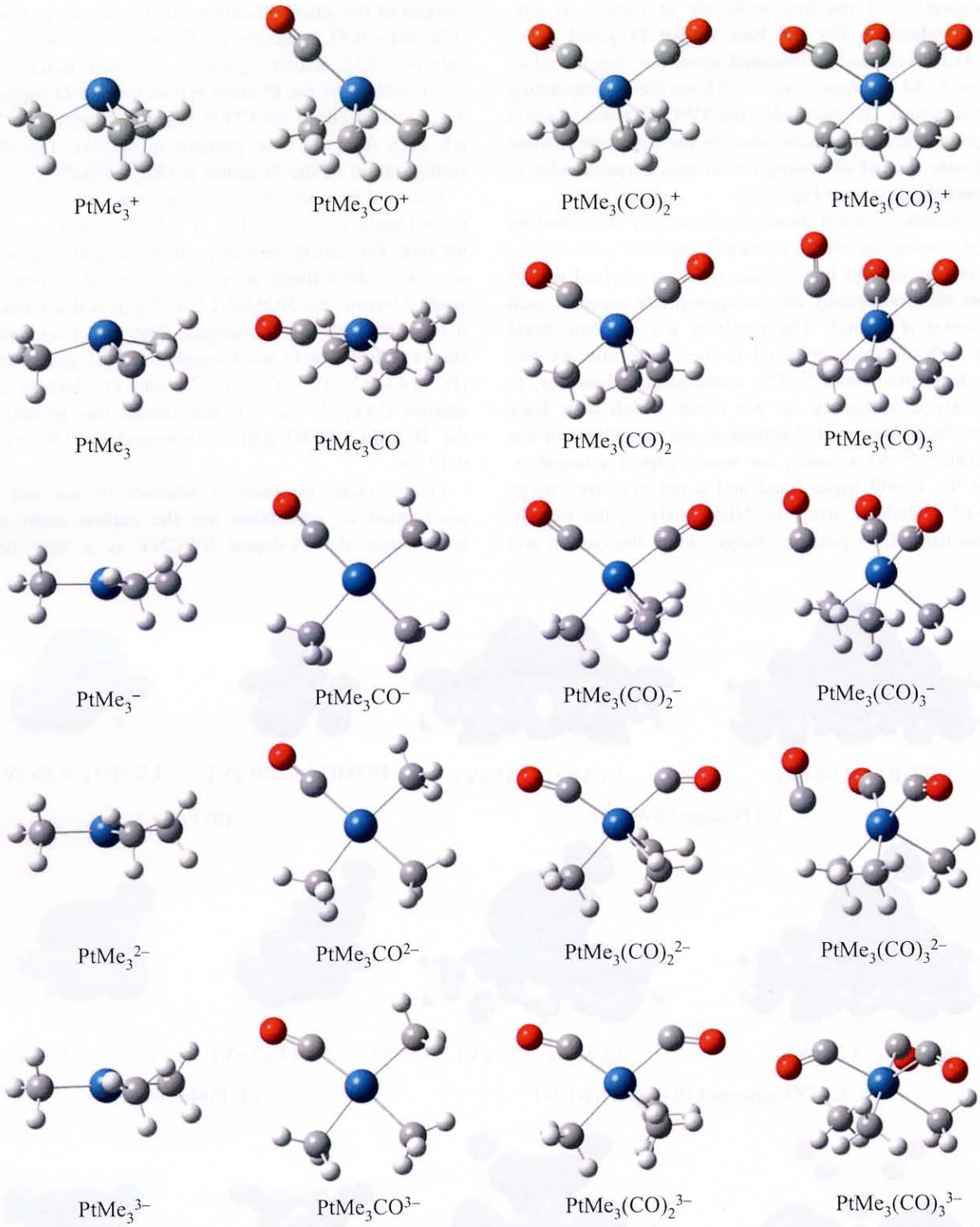

Fig. 3. Optimized geometries of alkylplatinum model compounds (grey = C, white = H, blue = Pt, red = O).

organometallic complex, reaction may take place in an unconventional O-binding mode. We attempted to probe at this possibility, and optimization of geometry resulted in a reasonable structure where the oxygen atom is close to the Pt center. Herein, we will refer to this complex as the OC-adsorbed Pt-doped SWCNT.

In this scenario, we observe less of a weakening of the C≡O bond and an increase in the distance from the Pt center to the CO molecule, suggesting a poorer interaction between the Pt-doped SWCNT and the adsorbate gas. Energy calculations also provide justification for this conclusion, as only 6.98 kcal/mol of energy is released upon

this adsorption for the singlet case, and 6.78 kcal/mol is liberated for the corresponding transformation for the triplet system. The net charge on the Pt atom is slightly higher, at 0.87 for the singlet and 0.89 for the triplet, due to less delocalization of electron density from the CO molecule as a result of the increased distance. The Pt electron configuration shows corresponding changes, $[Xe]6s^{0.46}5d^{8.67}$ for the singlet and $[Xe]6s^{0.41}5d^{8.70}$ for the triplet. The HOMO–LUMO gaps are now 0.66 and 0.41 eV for singlet and triplet states, respectively, again illustrating a smaller influence of CO on the electronic structure of the Pt-doped SWCNT with the reversed adsorption configuration.

3.3. Adsorption of Multiple CO Molecules

From the molecular orbitals shown in Figure 2(c) (and Fig. A4 in the appendix), one would expect that interaction with an additional CO molecule should be possible. A second adsorption should result in further stabilization as the coordination sites on the Pt center are becoming more saturated (note that Pt complexes can typically host up to six coordination ligands[40,42]). Because the coordination of the oxygen end of CO is less energetically favorable, we only studied C-binding adsorption.

We successfully identified a structure where two molecules of carbon monoxide are adsorbed (Fig. 1(d)). The overall energy released as a result of gas adsorption is 73.67 kcal/mol for the singlet system and 68.48 kcal/mol for the triplet, an average of 36.83 and 34.24 kcal/mol per CO adsorption, respectively. These values are slightly below those for the adsorption of a single CO molecule, not unexpected due to the increased steric crowding around the Pt atom.

The two CO molecules are almost identical in every aspect. The distance from the Pt atom to either of the CO molecules is 2.00 Å (ca. 1.97 Å for the monoadsorbed species), signifying weaker interaction between the metal and adsorbate. The carbon–oxygen separation for both molecules is 1.19 Å (slightly shorter than that of the monoadsorbed species). Once again, the charge on the Pt atom does not change to a significant degree (0.83), but the back donation to each CO has decreased (−0.05 charge on each CO, compared to −0.12 for the monoadsorbed species). The Pt electron configuration is now $[Xe]6s^{0.47}5d^{8.69}$, almost unaltered from before. The triplet state is almost identical in geometry. The HOMO–LUMO gaps are now 0.78 and 0.74 eV for singlet and triplet states, respectively. In comparison to the bare Pt-doped SWCNT, we observe larger HOMO–LUMO gaps.

All attempts to coordinate three CO molecules to the Pt-doped SWCNT were unsuccessful, likely due to the increased steric bulk of the nanotube ligand.

3.4. Comparison to Alkylplatinum Complexes

We decided to compare our systems with classical alkylplatinum species to gain some insight into the chemical reactivity of these novel nanotube-coordinated organometallic platinum complexes. Such alkylplatinum systems have been previously reported in the literature.[43–52] From Figure 1(d), it is evident that two of the three adjacent carbon atoms in the SWCNT are closer to the Pt atom than the last one, forming a pseudo-square planar geometry with the two CO molecules. This type of arrangement is well precedented in the literature,[23–25] although such complexes usually exhibit formal d^8 configuration (i.e., Pt^{2+}).[40,42] Hence, we examined a range of alkylplatinum complexes with oxidation state ranging between 0 and 4.

Recall that Jahn-Teller distortions occur for organometallic compounds where there is a degenerate set of orbitals that are unequally filled with valence electrons.[42] Thus, for these alkylplatinum complexes, we observe a strong dependence of geometry on the oxidation state of the Pt atom. It appears that the most appropriate model is $PtMe_3(CO)_x^+$, where the integral value of x ranges between 0 and 3 (Fig. 3). A comparison between the main properties of these species is given in Table I.

Unlike the Pt-doped SWCNTs, $PtMe_3^+$ is able to adsorb three CO molecules to form a six-coordinate platinum

Table I. Summary data for model compounds and nanotube-adsorbate complexes.

Species	ΔE^a	d(PtC)^b	d(CO)^c	q(Pt)^d	q(CO)^e	q(C)^f
$PtMe_3^+$	0			0.83		−2.13
$PtMe_3(CO)^+$	−28.11	2.04	1.17	0.84	0.09	−2.22
$PtMe_3(CO)_2^+$	−55.41	2.05, 2.05	1.17, 1.17	0.79	0.14, 0.14	−2.34
$PtMe_3(CO)_3^+$	−81.90	2.05, 2.05, 2.05	1.17, 1.17, 1.17	0.74	0.17, 0.17, 0.17	−2.47
Pt-doped $SWCNT_s^g$	0			0.82		−0.41
CO-adsorbed Pt-doped $SWCNT_s^g$	−41.23	1.97	1.19	0.85	−0.12	−0.43
$(CO)_2$-adsorbed Pt-doped $SWCNT_s^g$	−73.67	2.00, 2.00	1.19, 1.19	0.83	−0.05, −0.05	−0.49
Pt-doped $SWCNT_t^h$	0			0.84		−0.49
CO-adsorbed Pt-doped $SWCNT_t^h$	−33.09	1.96	1.20	0.83	−0.15	−0.46
$(CO)_2$-adsorbed Pt-doped $SWCNT_t^h$	−58.95	2.00, 2.00	1.19, 1.19	0.78	−0.02, −0.02	−0.49

[a]Total stabilization energy (in kcal/mol). [b]Distance (in Å) between Pt and C of CO. [c]Distance (in Å) between C and O of CO. [d]Partial charge on Pt. [e]Net partial charge on CO. [f]Net partial charge on the C atoms adjacent to Pt. [g]Singlet. [h]Triplet.

species. As mentioned before, the limitation of two CO molecules for the Pt-doped SWCNT is likely due to sterics but a molecular orbital analysis suggests that electronic factors may also play a role. By comparing the relevant FMOs (Fig. 2), we see that for both the bare Pt and mono-adsorbed species, a similarity exists between the Pt-doped SWCNT and the alkylplatinum complex. However, the orbitals appear to be quite different for the biadsorbed species, especially concerning the apparent lack of electron density around the metal center for the Pt-doped SWCNT HOMO. This may decrease the amount of back donation to the π-accepting CO ligands and hence diminish a stable $(CO)_3$-adsorbed Pt-doped SWCNT.

Also, it is evident that the negative charge on each methyl group in $PtMe_3^+$ is highly localized due to the lack of an extended carbon network in the immediate vicinity. On the other hand, the SWCNT has a large aromatic sidewall surface over which electron density can be spread, thus diminishing the localized negative charge on the carbon atoms directly attached to the Pt center. This changes the affinity for adsorbates since the back donating capability of the Pt atom is altered and further explains why a nanotube-adsorbate complex with three CO molecules is not stable.

4. CONCLUSIONS

We have reported the first computational study towards a new area of chemistry—nanotube-coordinated metal complexes. By fixing a metal atom on the sidewall of a SWCNT, we have shown novel chemical reactivity can result, differing but analogous to that of classical organometallic complexes. Adsorption of CO molecules on the Pt atom of the Pt-doped SWCNT is exothermic and forms a new class of nanotube-coordinated species. Further investigations in this area are ongoing to develop the fundamental chemistry of these complexes.

APPENDIX

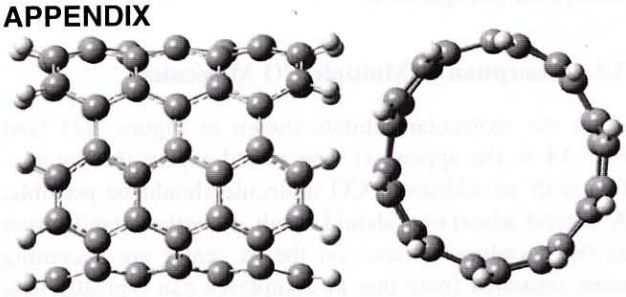

(a) View perpendicular to nanotube axis (b) View along nanotube axis

Fig. A1. Optimized geometry for the (5,5) SWCNT.

Table A1. Summary data for model compounds and nanotube-adsorbate complexes.

Species	ΔE^a	$d(PtC)^b$	$d(CO)^c$	$q(Pt)^d$	$q(CO)^e$	$q(C)^f$
$PtMe_3^+$	0			0.83		−2.13
$PtMe_3(CO)^+$	−28.11	2.04	1.17	0.84	0.09	−2.22
$PtMe_3(CO)_2^+$	−55.41	2.05, 2.05	1.17, 1.17	0.79	0.14, 0.14	−2.34
$PtMe_3(CO)_3^+$	−81.90	2.05, 2.05, 2.05	1.17, 1.17, 1.17	0.74	0.17, 0.17, 0.17	−2.47
$PtMe_3$	0			0.60		−2.63
$PtMe_3(CO)$	−41.19	1.93	1.19	0.68	−0.05	−2.71
$PtMe_3(CO)_2$	−63.47	1.96, 1.96	1.19, 1.19	0.75	−0.05, −0.05	−2.70
$PtMe_3(CO)_3$	−70.64	1.98, 1.98, 2.40	1.19, 1.19, 1.20	0.75	0.00, 0.00, −0.17	−2.65
$PtMe_3^-$	0			0.31		−3.01
$PtMe_3(CO)^-$	−64.41	1.87	1.21	0.53	−0.17	−3.18
$PtMe_3(CO)_2^-$	−67.27	1.91, 1.92	1.21, 1.22	0.77	−0.25, −0.35	−3.03
$PtMe_3(CO)_3^-$	−77.30	1.92, 1.93, 2.97	1.20, 1.21, 1.21	0.76	−0.27, −0.22, −0.22	−2.94
$PtMe_3^{2-}$	0			−0.48		−3.10
$PtMe_3(CO)^{2-}$	−66.81	1.88	1.23	−0.15	−0.40	−3.20
$PtMe_3(CO)_2^{2-}$	−86.15	1.91, 2.03	1.25, 1.25	0.65	−0.55, −0.56	−3.24
$PtMe_3(CO)_3^{2-}$	−107.55	1.98, 2.00, 2.72	1.23, 1.24, 1.24	0.65	−0.43, −0.44, −0.45	−3.11
$PtMe_3^{3-}$	0			−1.57		−3.02
$PtMe_3(CO)^{3-}$	−71.74	1.88	1.23	−1.12	−0.38	−3.19
$PtMe_3(CO)_2^{3-}$	−93.82	1.91, 2.08	1.26, 1.26	0.08	−0.60, −0.73	−3.36
$PtMe_3(CO)_3^{3-}$	−130.61	2.14, 2.15, 2.15	1.25, 1.26, 1.26	0.21	−0.55, −0.55, −0.55	−3.25
Pt-doped $SWCNT_s^g$	0			0.82		−0.41
CO-adsorbed Pt-doped $SWCNT_s^g$	−41.23	1.97	1.19	0.85	−0.12	−0.43
$(CO)_2$-adsorbed Pt-doped $SWCNT_s^g$	−73.67	2.00, 2.00	1.19, 1.19	0.83	−0.05, −0.05	−0.49
Pt-doped $SWCNT_t^h$	0			0.84		−0.49
CO-adsorbed Pt-doped $SWCNT_t^h$	−33.09	1.96	1.20	0.83	−0.15	−0.46
$(CO)_2$-adsorbed Pt-doped $SWCNT_t^h$	−58.95	2.00, 2.00	1.19, 1.19	0.78	−0.02, −0.02	−0.49

[a]Total stabilization energy (in kcal/mol). [b]Distance (in Å) between Pt and C of CO. [c]Distance (in Å) between C and O of CO. [d]Partial charge on Pt. [e]Net partial charge on CO. [f]Net partial charge on the C atoms adjacent to Pt. [g]Singlet. [h]Triplet.

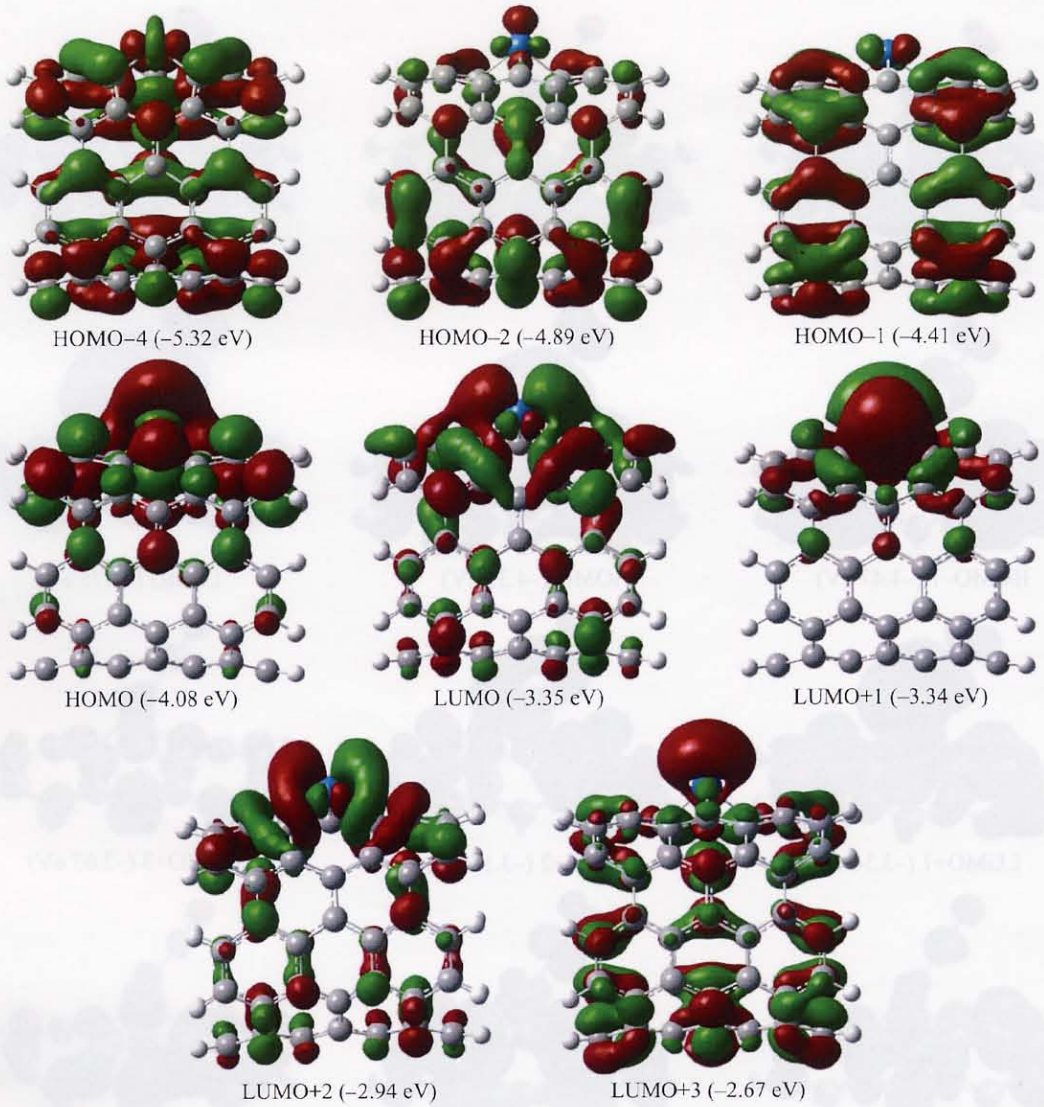

Fig. A2. Relevant molecular orbitals for the ground state Pt-doped SWCNT. HOMO $- n$ (p eV) is the nth orbital below the HOMO with orbital energy p eV. LUMO $+ m$ (q eV) is the mth orbital above the LUMO with orbital energy q eV.

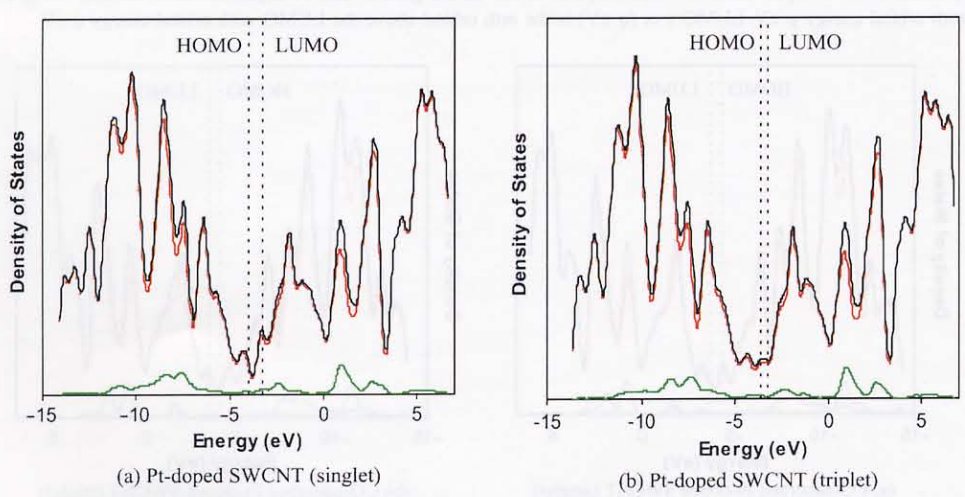

Fig. A3. LDOS (red = carbon framework, green = Pt) and DOS (black) of the Pt-doped SWCNT.

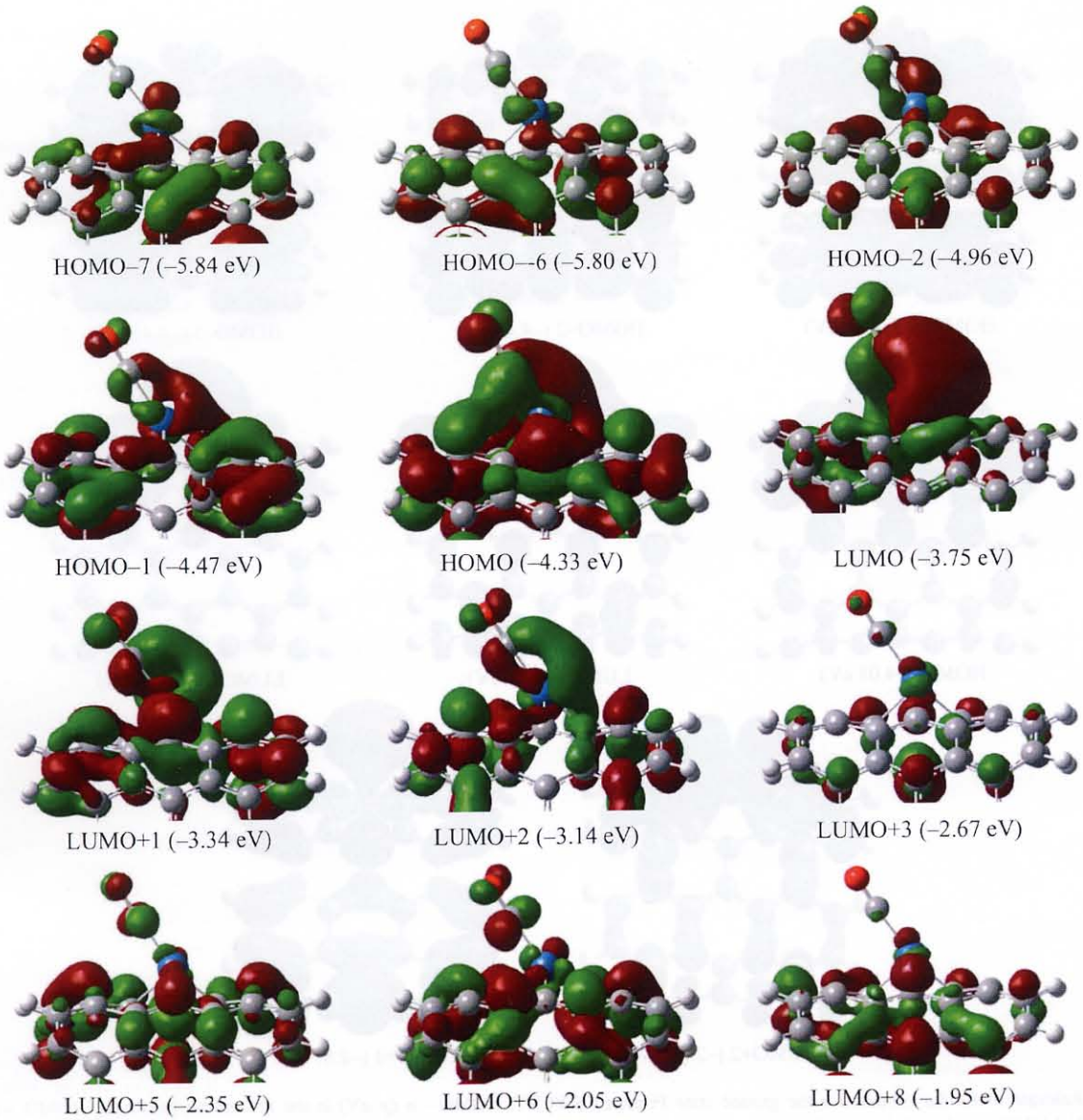

Fig. A4. Partial molecular orbitals important to the chemisorption of CO on the ground state Pt-doped SWCNT. HOMO $- n$ (p eV) is the nth orbital below the HOMO with orbital energy p eV. LUMO $+ m$ (q eV) is the mth orbital above the LUMO with orbital energy q eV.

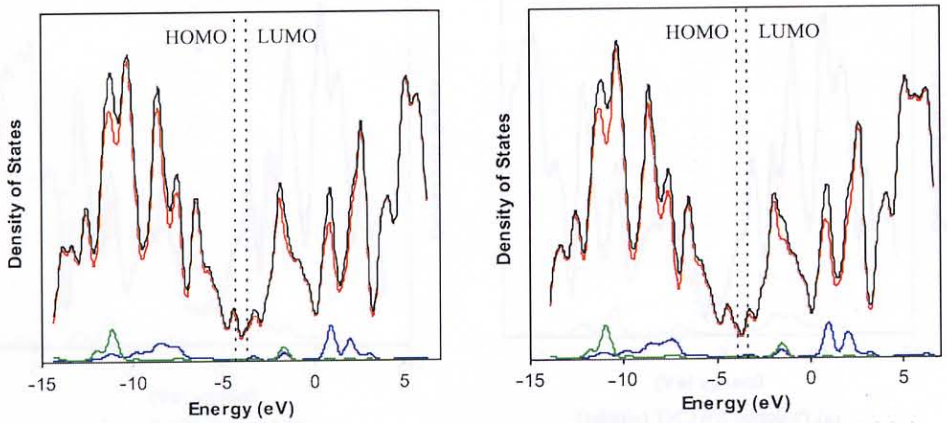

(a) CO-adsorbed Pt-doped SWCNT (singlet) (b) CO-adsorbed Pt-doped SWCNT (triplet)

Fig. A5. LDOS (red = carbon framework, green = Pt, blue = CO) and DOS (black) for the CO-adsorbed Pt-doped SWCNT.

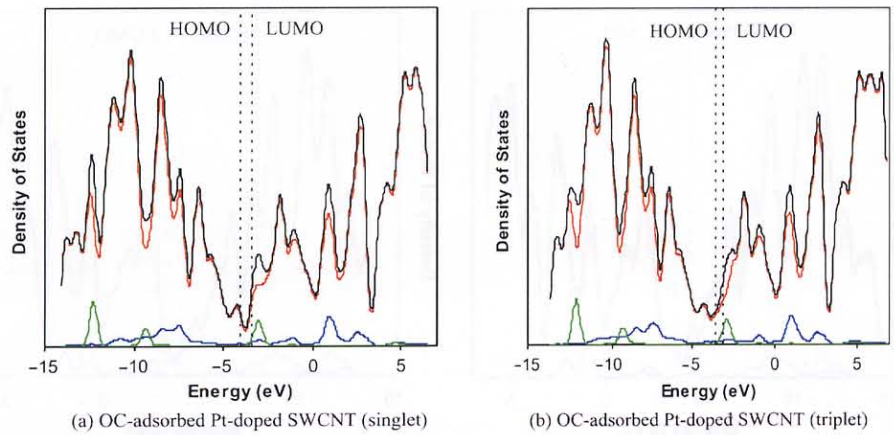

(a) OC-adsorbed Pt-doped SWCNT (singlet) (b) OC-adsorbed Pt-doped SWCNT (triplet)

Fig. A6. LDOS (red = carbon framework, green = Pt, blue = CO) and DOS (black) for the OC-adsorbed Pt-doped SWCNT.

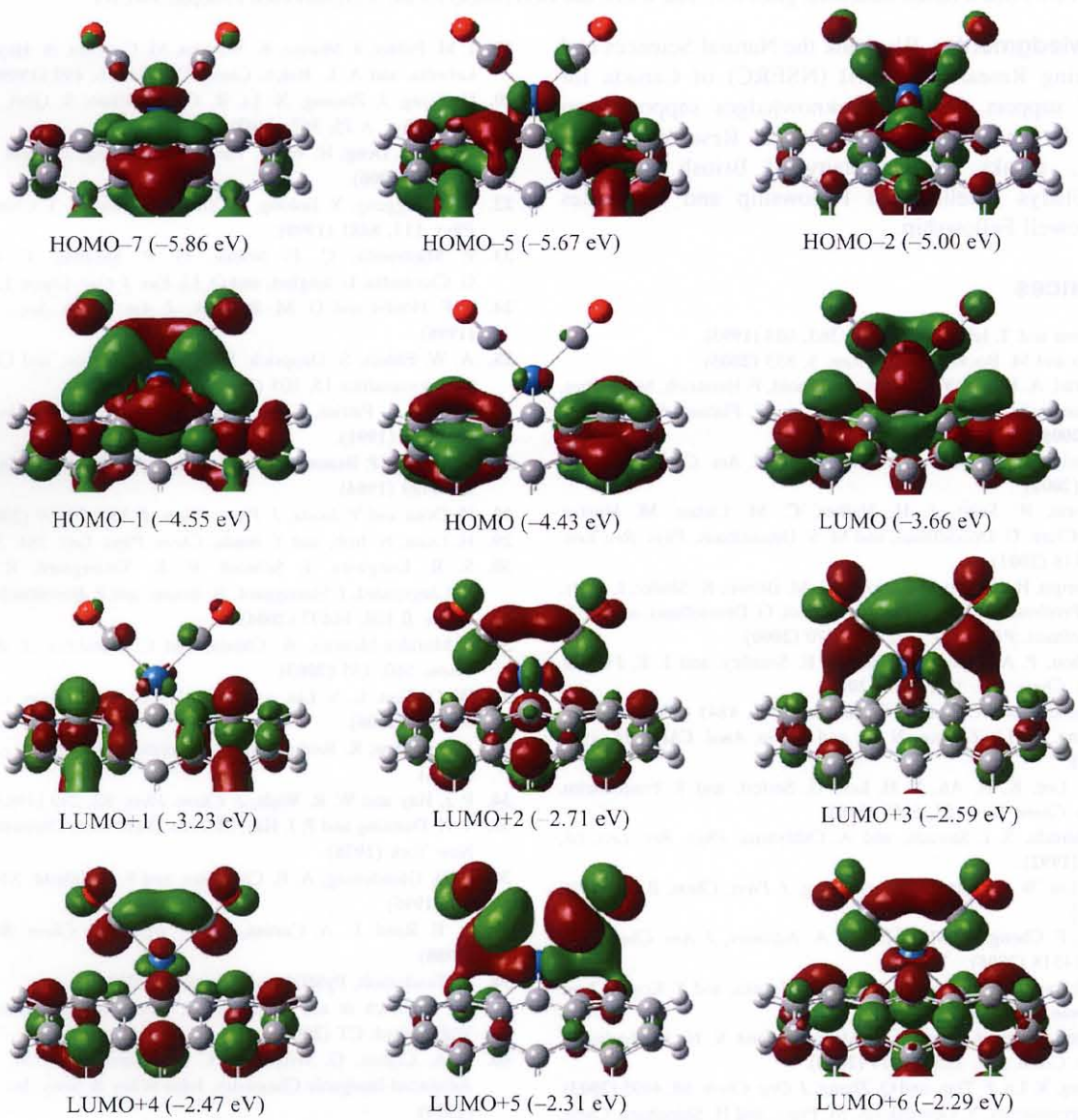

Fig. A7. Partial molecular orbitals important to chemisorption of two CO molecules on the ground state Pt-doped SWCNT. HOMO $- n$ (p eV) is the nth orbital below the HOMO with orbital energy p eV. LUMO $+ m$ (q eV) is the mth orbital above the LUMO with orbital energy q eV.

RESEARCH ARTICLE

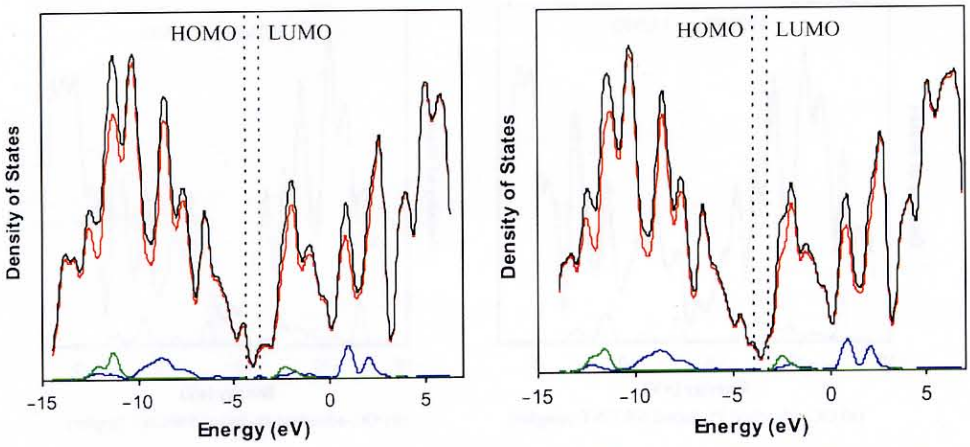

(a) $(CO)_2$-adsorbed Pt-doped SWCNT (singlet) (b) $(CO)_2$-adsorbed Pt-doped SWCNT (triplet)

Fig. A8. LDOS (red = carbon framework, green = Pt, blue = CO) and DOS (black) for the $(CO)_2$-adsorbed Pt-doped SWCNT.

Acknowledgments: We thank the Natural Sciences and Engineering Research Council (NSERC) of Canada for financial support. C. S. Y. acknowledges support from NSERC for an Undergraduate Student Research Award. L. V. L. thanks the University of British Columbia for a Gladys Estella Laid Fellowship and a Charles A. McDowell Fellowship.

References

1. S. Iijima and T. Ichihashi, *Nature* 363, 603 (**1993**).
2. J. Heo and M. Bockrath, *Nano Lett.* 5, 853 (**2005**).
3. T. Hertel, A. Hagen, V. Talalaev, K. Arnold, F. Hennrich, M. Kappes, S. Rosenthal, J. McBride, H. Ulbricht, and E. Flahaut, *Nano Lett.* 5, 511 (**2005**).
4. J. Cioslowski, N. Rao, and D. Moncrieff, *J. Am. Chem. Soc.* 124, 8485 (**2002**).
5. A. Jorio, R. Saito, J. H. Hafner, C. M. Lieber, M. Hunter, T. McClure, G. Dresselhaus, and M. S. Dresselhaus, *Phys. Rev. Lett.* 86, 1118 (**2001**).
6. K. Kneipp, H. Kneipp, P. Corio, S. D. M. Brown, K. Shafer, J. Motz, L. T. Perelman, E. B. Hanlon, A. Marucci, G. Dresselhaus, and M. S. Dresselhaus, *Phys. Rev. Lett.* 84, 3470 (**2000**).
7. W. Zhou, P. A. Heiney, H. Fan, R. E. Smalley, and J. E. Fischer, *J. Am. Chem. Soc.* 127, 1640 (**2005**).
8. J. Rajendra and A. Rodger, *Chem. Eur. J.* 11, 4841 (**2005**).
9. J. Wang, M. Li, Z. Shin, N. Li, and Z. Gu, *Anal. Chem.* 74, 1993 (**2002**).
10. S. M. Lee, K. H. An, Y. H. Lee, G. Seifert, and T. Frauenheim, *J. Am. Chem. Soc.* 123, 5059 (**2001**).
11. N. Hamada, S.-I. Sawada, and A. Oshiyama, *Phys. Rev. Lett.* 68, 1579 (**1992**).
12. L. V. Liu, W. Q. Tian, and Y. A. Wang, *J. Phys. Chem. B* 110, 1999 (**2006**).
13. H. Li, F. Cheng, A. M. Duft, and A. Adronov, *J. Am. Chem. Soc.* 127, 14518 (**2005**).
14. T. Nakamura, M. Ishihara, T. Ohana, A. Tanaka, and Y. Koga, *Chem. Commun.* 1336 (**2004**).
15. H. Peng, L. B. Alemay, J. L. Margrave, and V. N. Khabashesku, *J. Am. Chem. Soc.* 125, 15174 (**2003**).
16. L. Long, X. Lu, F. Tian, and Q. Zhang, *J. Org. Chem.* 68, 4495 (**2003**).
17. N. Tagmatarchis, V. Georgakilas, M. Prato, and H. Shinohara, *Chem. Commun.* 2010 (**2002**).
18. W. Branz, I. M. L. Billas, N. Malinowski, F. Tast, M. Heinebrodt, and T. P. Martin, *J. Chem. Phys.* 109, 3425 (**1998**).
19. J. M. Poblet, J. Munoz, K. Winkler, M. Cancilla, A. Hayashi, C. B. Lebrilla, and A. L. Balch, *Chem. Commun.* 6, 493 (**1999**).
20. Q. Kong, J. Zhuang, X. Li, R. Cai, L. Zhao, S. Qian, and Y. Li, *Appl. Phys. A* 75, 367 (**2002**).
21. G. Lu, K. Deng, H. Wu, J. Yang, and X. Wang, *J. Chem. Phys.* 124, 054305 (**2006**).
22. D. Changgeng, Y. Jinlong, C. Xiangyuan, and C. T. Chan, *J. Chem. Phys.* 111, 8481 (**1999**).
23. P. Mastrorilli, C. F. Nobile, G. P. Suranna, F. P. Fanizzi, G. Ciccarella, U. Englert, and Q. Li, *Eur. J. Org. Chem.* 1234 (**2004**).
24. J. F. Houlis and D. M. Roddick, *J. Am. Chem. Soc.* 120, 11020 (**1998**).
25. A. W. Ehlers, S. Dapprich, S. F. Vyboishchikov, and G. Frenking, Organometallics 15, 105 (**1996**).
26. J. Puga, R. Patrini, K. M. Sanchez, and B. C. Gates, *Inorg. Chem.* 30, 2479 (**1991**).
27. R. Bender, P. Braunstein, J.-M. Jud, and Y. Dusausoy, *Inorg. Chem.* 23, 4489 (**1984**).
28. H. Orita and Y. Inada, *J. Phys. Chem. B* 109, 22469 (**2005**).
29. H. Orita, N. Itoh, and Y. Inada, *Chem. Phys. Lett.* 384, 271 (**2004**).
30. S. R. Longwitz, J. Schnadt, E. K. Vestergaard, R. T. Vang, E. Laegsgaard, I. Stensgaard, H. Brune, and F. Besenbacher, *J. Phys. Chem. B* 108, 14497 (**2004**).
31. I. Morales-Moreno, A. Cuesta, and C. Gutiérrez, *J. Electroanal. Chem.* 560, 135 (**2003**).
32. W. Q. Tian, L. V. Liu, and Y. A. Wang, *Phys. Chem. Chem. Phys.* 8, 3528 (**2006**).
33. J. P. Perdew, K. Burke, and M. Ernzerhof, *Phys. Rev. Lett.* 77, 3865 (**1996**).
34. P. J. Hay and W. R. Wadt, *J. Chem. Phys.* 82, 299 (**1985**).
35. T. H. Dunning and P. J. Hay, Modern Theoretical Chemistry, Plenum, New York (**1976**).
36. E. D. Glendening, A. E. Carpenter, and F. Weinhold, NBO, Version 3.1 (**1995**).
37. A. E. Reed, L. A. Curtiss, and F. Weinhold, *Chem. Rev.* 88, 899 (**1988**).
38. A. Tenderholt, PyMOlyze, Version 1.1 (**2005**).
39. M. J. Frisch et al., Gaussian 03, Revision B.05, Gaussian, Inc., Wallingford, CT (**2004**).
40. F. A. Cotton, G. Wilkinson, C. A. Murillo, and M. Bochmann, Advanced Inorganic Chemistry, John Wiley & Sons, Inc., New York (**1999**).
41. G. Blyholder, *J. Phys. Chem.* 68, 2772 (**1964**).
42. C. E. Housecroft and A. G. Sharpe, Inorganic Chemistry, Pearson Education Limited, Essex, England (**2001**).

43. C. R. Baar, H. A. Jenkins, J. J. Vittal, G. P. A. Yap, and R. J. Puddephatt, *Organometallics* 17, 2805 (**1998**).
44. M. Fusto, F. Giordano, I. Orabona, and F. Ruffo, *Organometallics* 16, 5981 (**1997**).
45. L. Wang, S. S. Stahl, J. A. Labinger, and J. E. Bercaw, *J. Molec. Catal. A* 116 (**1997**).
46. S. S. Stahl, J. A. Labinger, and J. E. Bercaw, *J. Am. Chem. Soc.* 118, 5961 (**1996**).
47. M. L. Ferrara, I. Orabona, F. Ruffo, and V. D. Felice, *J. Organomet. Chem.* 519, 75 (**1996**).
48. S. S. Stahl, J. A. Labinger, and J. E. Bercaw, *J. Am. Chem. Soc.* 117, 9371 (**1995**).
49. D. L. Reger, J. C. Baxter, and D. G. Garza, *Organometallics* 9, 16 (**1990**).
50. G. Alibrandi, M. Cusumano, D. Minniti, L. M. Scolaro, and R. Romeo, *Inorg. Chem.* 28, 342 (**1989**).
51. T. M. Miller, A. N. Izumi, Y.-S. Shih, and G. M. Whitesides, *J. Am. Chem. Soc.* 110, 3146 (**1988**).
52. R. DiCosimo, S. S. Moore, A. F. Sowinski, and G. M. Whitesides, *J. Am. Chem. Soc.* 104, 124 (**1982**).

Received: 31 October 2006. Accepted: 4 November 2006.

RESEARCH ARTICLE